FULL PAPER

ADVANCED FUNCTIONAL MATERIALS

Synthesis and Crystal Growth of Stilbazolium Derivatives for Second-Order Nonlinear Optics

By *Zhou Yang*,* *Shanmugam Aravazhi*, *Arno Schneider*, *Paul Seiler*, *Mojca Jazbinsek*, and *Peter Günter*

A series of ionic stilbazolium salts with benzenesulfonates with different substituents in the *para* position have been synthesized. Single crystals of 4-*N*,*N*-dimethylamino-4′-*N*′-methylstilbazolium *p*-methoxybenzenesulfonate (DSMOS) were successfully grown in methanol solution by slow cooling. X-ray studies revealed that DSMOS crystallized in the triclinic space group *P*1 with its molecular dipoles perfectly aligned in one direction—favorable for large nonlinear optical and electro-optical effects. Kurtz powder tests revealed a large powder second-harmonic generation efficiency that is similar to that of the well-studied 4-*N*,*N*-dimethylamino-4′-*N*′-methylstilbazolium tosylate (DAST).

1. Introduction

Organic nonlinear optical materials are of increasing interest because of their potential for applications in high-speed and high-density data processing, storage, and telecommunications.[1–3] Well-designed organic nonlinear optical materials may be far superior to their inorganic counterparts, owing to their relatively high and much faster nonlinearities. Among the various classes of materials investigated worldwide, ionic organic crystals are of special interest due to their advantageous mechanical, chemical, and thermal properties.[4,5] Among them, DAST (4-*N*,*N*-dimethylamino-4′-*N*′-methylstilbazolium tosylate) is well-known because of its large nonlinear optical susceptibility (d) and electro-optic coefficient (r).[6,7] We have studied the growth of DAST crystals, its processing, and device applications for the last several years.[8,9] The results show that DAST promises to work well for highly efficient, high-speed electro-optic applications. The growth of bulk, high-quality DAST crystals from solution, however, remains extremely difficult, requiring temperature stabilities within ±0.002 °C over several months. Therefore it is desirable to develop organic crystals, with similar nonlinear optical properties, that are both easier and quicker to grow. Based on the excellent nonlinear optical properties of DAST, new organic nonlinear crystals—based on strong Coulomb interactions to induce highly non-centrosymmetric and stable packing—are being developed. Research shows that the counter-anion plays an important role in achieving a non-centrosymmetric structure in ionic organic crystals.[4,5] For example, the large second-harmonic generation (SHG) activity of DAST has been interpreted as resulting from the tetrahedral sulfonate group of tosylate.[4] However, the effect of the *p*-substituent of the counter-anion has not yet been fully studied.

Herein, we report the synthesis, crystal growth, and characterisation of a series of stilbazolium derivatives, obtained by carefully modifying the structure with various *p*-substituents on the counter-anion, expecting new molecules with high second-order optical nonlinearities. Two of the four salts we synthesized have SHG intensities that are comparable to that of DAST. This indicates that the *p*-substituent on the counter-anion plays an important role in the crystal structure and SHG activity of organic materials. The present study forms a basis for optimizing DAST-like structures to improve their second-order nonlinear optical properties, thermal stability, and crystal-growing ability.

2. Results and Discussion

2.1. Synthesis and Characterization

Four kinds of stilbazolium derivatives with *p*-hydroxyl, *p*-methoxyl, *p*-amino, and *p*-dimethylamino on the counter-anions have been prepared. The chemical structures of these stilbazolium derivatives are shown in Scheme 1, together with their abbreviations. Compounds 4-*N*,*N*-dimethylamino-4′-*N*′-methylstilbazolium *p*-hydroxybenzenesulfonate (DSHS), 4-*N*,*N*-dimethylamino-4′-*N*′-methylstilbazolium *p*-aminobenzenesulfonate (DSAS), and 4-*N*,*N*-dimethylamino-4′-*N*′-methylstilbazolium *p*-dimethylaminobenzenesulfonate (DSMAS) were prepared

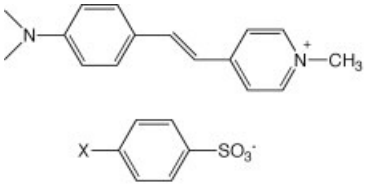

X	Abbr.
OH	DSHS
OCH_3	DSMOS
NH_2	DSAS
$N(CH_3)_2$	DSMAS
CH_3	DAST

Scheme 1. Structures of the stilbazolium derivatives and their abbreviations.

[*] Dr. Z. Yang, Dr. S. Aravazhi, A. Schneider, Dr. M. Jazbinsek, Prof. P. Günter
Nonlinear Optics Laboratory, Institute of Quantum Electronics
ETH Hönggerberg
CH-8093 Zürich (Switzerland)
E-mail: zhouyang@phys.ethz.ch
P. Seiler
Laboratory of Organic Chemistry, ETH Hönggerberg
CH-8093 Zürich (Switzerland)

 © 2005 WILEY-VCH Verlag GmbH & Co. KGaA, Weinheim DOI: 10.1002/adfm.200500036

ADVANCED FUNCTIONAL MATERIALS

by metathesization of the iodide salt with the sodium salt of the corresponding anion, as described previously.[10] 4-*N*,*N*-Dimethylamino-4′-*N*′-methylstilbazolium *p*-methoxybenzenesulfonate (DSMOS) was synthesized by a condensation reaction of 4-methyl-*N*-methyl pyridinium *p*-methoxybenzenesulfonate, which was prepared from 4-picoline and *p*-methoxybenzenesulfonate, and 4-*N*,*N*-dimethylaminobenzenehyde in the presence of piperidine. *p*-Methoxybenzenesulfonate was synthesized by the method described by Carr and Brown.[11]

The melting point, UV absorption peak λ_{max}, and solubility of these new compounds and DAST are listed in Table 1. All four new compounds have high melting points—above 250 °C. The melting points of DSHS, DSMOS, and DSAS are 8–18 °C higher than DAST. The melting point of DSMAS is about the same as that of DAST. In comparison with DSMOS and DSMAS, which possess methyl substituents, DSHS and DSAS have melting points that are higher by 10 and 16 °C, respectively. The presence of intermolecular hydrogen bonding between the hydroxyl or amino and sulfonate groups should be one of the factors contributing to their high melting points.

Table 1. Physical properties of the investigated compounds and DAST.

Compound	Melting Point [°C]	λ_{max} [a] [nm]	Solubility [b] [g 100 g^{-1}]
DSHS	274 ± 1	474	1.0
DSMOS	264 ± 1	476	2.7
DSAS	272 ± 1	476	1.1
DSMAS	256 ± 1	474	2.4
DAST	256 ± 1	475	4.5

[a] In methanol at room temperature. [b] In methanol at 48 °C.

The λ_{max} values in the UV-vis spectra of these compounds are nearly the same as that of DAST. This is because, in the visible region, λ_{max} is determined by the cation in the methanol solution: The change in the *p*-substituted group of the counter-anion does not affect the electronic structure of the stilbazolium cation.

DAST is barely soluble in non-polar and most polar solvents, with the exception of alcohol. The most suitable solvent for crystallizing DAST is methanol.[8] DSHS and DSAS, possessing hydroxyl and amino groups, are not readily soluble, even in methanol. A higher solubility was achieved by introducing alkyl substitution, as in DSMOS and DSMAS. The solubility of DSMOS in methanol was measured as a function of temperature (Fig. 1). The typical increase in solubility with increasing temperature shows that methanol is a suitable solvent for growing DSMOS crystals.

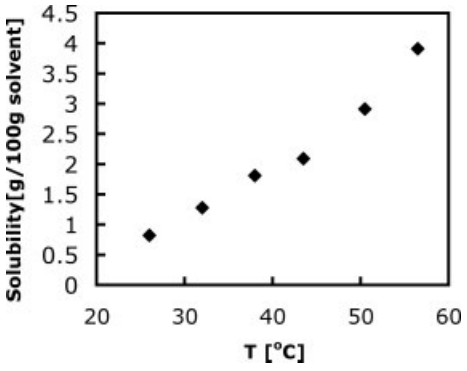

Figure 1. The solubility/temperature behavior of DSMOS in methanol.

2.2. Kurtz Powder Test Studies

The relative SHG activities of the stilbazolium compounds and DAST were measured using the Kurtz powder technique[12] as the standard technique for screening the nonlinear optical activity of the new compounds. An idler wave at a wavelength of 1907 nm, from an optical parametric amplifier, pumped by an amplified Ti:sapphire laser was used to determine the nonresonant SHG efficiency. Of the four compounds (DSHS, DSMOS, DSAS, and DSMAS), DSMOS, DSAS, and DSMAS exhibited strong second-harmonic signals in the powder test. Using ground powder, without controlling the powder size, we obtained SHG efficiencies of 0.9, 1.0, and 0.7 times that of DAST for DSMOS, DSAS, and DSMAS, respectively. Therefore, the SHG activities of DSMOS and DSAS seem to be similar to DAST, considering the uncertainty (10–40 %) in the measured SHG conversion efficiencies of unsized powders. Since DSAS and DSMAS possess similar structures, it is likely that the lower SHG efficiency of the latter is mostly due to the larger size of the *p*-dimethylamino substituent of the counter-anion.

2.3. Crystal Growth and X-ray Crystallographic Study

The synthesized salts (DSMOS, DSAS, and DSMAS) that possessed strong second-harmonic signals were of interest for crystal-growth experiments. Slow cooling was adapted for the growth. DSMOS nucleated more easily than DSAS and DSMAS; the crystal yield was also higher. Small red crystals in the shape of thin plates, typically 3 mm × 5 mm × 0.3 mm in size, were obtained in two weeks (Fig. 2).

We investigated the optical quality of the crystals by placing them between crossed polarizers (Fig. 3). When the crystal was rotated around the direction of the light propagation, the linear-

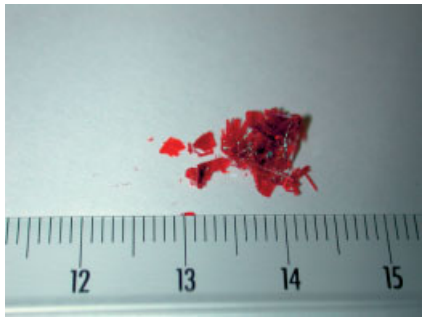

Figure 2. DSMOS crystals grown by slow cooling.

 © 2005 WILEY-VCH Verlag GmbH & Co. KGaA, Weinheim

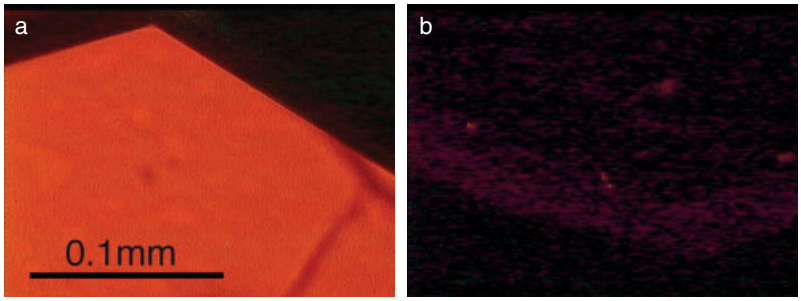

Figure 3. DSMOS crystal (30 μm thick) as observed between the crossed polarizers in a microscope. The crystal was rotated 45° from position (a) to position (b).

ly polarized light was transmitted when its polarization was neither parallel nor perpendicular to an axis of the optical indicatrix. The crystal appears completely opaque when at least one of the polarizers is parallel to an axis of the optical indicatrix. For polycrystals, some parts appear transparent while the others appear opaque during the rotation. Using this method, we were able to conclude that we produced single crystals with at least one of the main optical axes almost parallel to the plate.

It is well-known that three-dimensional crystal packing is extremely sensitive to subtle structural modifications. Even a minor change of a substituent may entirely alter the relative orientation and arrangement of the molecular assemblies, as well as the three-dimensional packing.[13] Compared with the large SHG efficiency and good crystal-growth ability of DSMOS, DSHS crystallizes in a centrosymmetric structure, thus showing no SHG efficiency; this change is achieved only by replacing the *p*-methoxyl group of the former with a *p*-hydroxyl group. In the case of DSAS and DSMAS, the crystal formation was very poor, giving only small needle-like crystals after one month. The poor crystal formation of DSAS and DSMAS can be explained as follows: i) In DSAS, poor crystallization is due to the low solubility in the methanol solvent; ii) In DSMAS, it is due to the bulky *p*-dimethylamino group of the counter-anion. Because of the large SHG activity of DSAS, crystal growth based on other methods is currently being investigated.

Single-crystal X-ray analysis was carried out on DSMOS crystals. The crystallographic data is listed in the Experimental section and Table 2, where DAST data is also added for comparison. The crystal is triclinic, possessing space group symmetry *P*1, with four ion-pairs per unit cell. The structure of one ion-pair is shown in Figure 4, and a packing diagram in Figure 5. The three-dimensional packing exhibits alternating acentric sheets of stilbazolium cations and *p*-methoxybenzenesulfonate anions. The observed parallel arrangement of all stilbazolium chromophores is a prerequisite for efficient electro-optic or second-order nonlinear optical effects. The tilting angle θ between the cation's long axis and the polar *a*-axis of the crystal is about 18°, giving an order parameter $\langle\cos^3\theta\rangle = 0.86$. In the case of DAST, θ has been reported to be 20° ($\langle\cos^3\theta\rangle = 0.83$).[6] Hence it is obvious that the component of the nonlinear optical susceptibility element *d* along the polar axis direction of DSMOS crystals can become slightly larger than that of DAST, provided that the hyperpolarizability of DSMOS remains the same. Therefore, a high second-order nonlinear optical coefficient, *d*, and electro-optic coefficient, *r*, are expected for DSMOS organic crystals.

Table 2. Crystallographic data of DSMOS and DAST crystals.

	DSMOS	DAST [6]
Formula	$C_{23}H_{26}N_2O_4S$	$C_{23}H_{26}N_2O_3S$
Formula weight	426.5	410.5
Crystal system	Triclinic	Monoclinic
Space group	*P*1	*Cc*
a [nm] [a]	1.06197(5)	1.0365(3)
b [nm]	1.10315(5)	1.1322(4)
c [nm]	1.85956(9)	1.7893(4)
α [°]	95.925	90
β [°]	103.647	92.24
γ [°]	92.174	90
V [nm^3]	2.10131	2.09821

[a] Values for DSMOS and DAST are converted to nanometers.

3. Conclusions

Four organic salts DSAS, DSHS, DSMOS, and DSMAS, based on minor structural modifications of the *p*-substituent of the counter-anion of stilbazolium salts have been synthesized. SHG Kurtz powder tests revealed that DSAS, DSMOS, and DSMAS possess non-centrosymmetric structures. DSAS and DSMOS crystals have been grown by the slow-cooling technique and show high SHG efficiencies, comparable with that of DAST. Crystal-growth experiments revealed that DSMOS can be crystallized more easily than DSAS and DSMAS. Single crystals of DSMOS with dimensions up to 3 mm × 5 mm × 0.3 mm and good optical quality have been grown. X-ray diffraction studies were carried out for DSMOS: the crystal belongs to the triclinic space group *P*1, with a parallel arrangement of all stilbazolium chromophores, which is promising for second-order nonlinear optical applications.

4. Experimental

Synthesis, General Considerations: All reagents were purchased at high purity (AR grade) from Aldrich and used without further purification. The products were dried under vacuum for 24 h to remove solvents effectively. ^{1}H NMR spectra were recorded on a Bruker 300 MHz spectrometer in deuterated dimethylsulfoxide (DMSO-d_6) solutions. UV-vis spectra were recorded by a Perkin-Elmer Lambda 9 spectrometer. Elemental analyses were performed by the Microanalytical Laboratory, ETH. Thermal analyses were conducted on a Perkin-Elmer TGA-7 and DSC-7 spectrometer at a heating rate of 10 °C min^{-1}.

4-N,N-Dimethylamino-4′-N′-methylstilbazolium p-hydroxybenzenesulfonate, DSHS: Yield 75 %; ^{1}H NMR (300 MHz, DMSO-d_6) δ [ppm]: 9.48 (s, 1H, OH), 8.68 (d, 2H, J = 6.9 Hz, C_5H_4N), 8.04 (d, 2H, J = 6.9 Hz, C_5H_4N), 7.92 (d, 1H, J = 16.0 Hz, CH), 7.60 (d, 2H, J = 8.8 Hz, C_6H_4), 7.40 (d, 2H, J = 8.1 Hz, $C_6H_4SO_3^-$), 7.18 (d, 1H, J = 15.9 Hz, CH), 6.79 (d, 2H, J = 8.1 Hz, $C_6H_4SO_3^-$), 6.66 (d, 2H, J = 8.9 Hz, C_6H_4), 4.16 (s, 3H,

 © 2005 WILEY-VCH Verlag GmbH & Co. KGaA, Weinheim

ADVANCED FUNCTIONAL MATERIALS

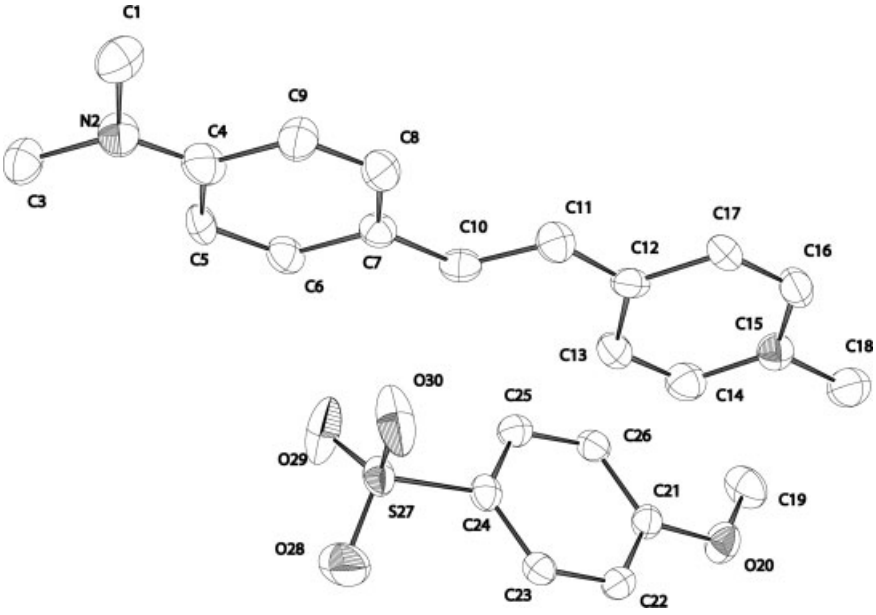

Figure 4. Oak Ridge thermal ellipsoid program (ORTEP) representation of one ion-pair of DSMOS at 263 K. (Vibrational ellipsoids are shown at the 30% probability level.)

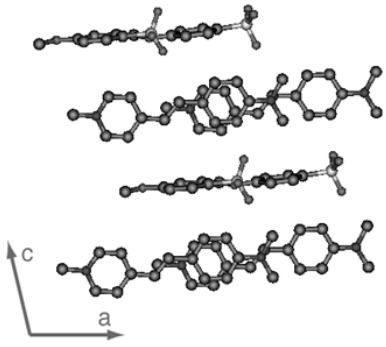

Figure 5. Crystal-packing diagram of DSMOS (projected on the *ac* plane).

Me), 3.02 (s, 6H, NMe_2). Anal. calcd. for $C_{22}H_{24}N_2O_4S$: C, 64.06; H, 5.86; N, 6.79. Found: C, 63.88; H, 5.95; N, 6.64.

4-N,N-Dimethylamino-4′-N′-methylstilbazolium p-methoxybenzenesulfonate, DSMOS: Yield 66%; ^{1}H NMR (300 MHz, DMSO-d_6) δ [ppm]: 8.67 (d, 2H, J = 6.6 Hz, C_5H_4N), 8.03 (d, 2H, J = 6.9 Hz, C_5H_4N), 7.91 (d, 1H, J = 16.2 Hz, CH), 7.58 (d, 2H, J = 8.7 Hz, C_6H_4), 7.50 (d, 2H, J = 8.7 Hz, $C_6H_4SO_3^-$), 7.17 (d, 1H, J = 16.2 Hz, CH), 6.83 (d, 2H, J = 8.7 Hz, $C_6H_4SO_3^-$), 6.78 (d, 2H, J = 8.9 Hz, C_6H_4), 4.15 (s, 3H, Me), 3.72 (s, 3H, OMe), 3.00 (s, 6H, NMe_2). Anal. calcd. for $C_{23}H_{26}N_2O_4S$: C, 64.77; H, 6.14; N, 6.57. Found: C, 64.95; H, 6.24; N, 6.57.

4-N,N-Dimethylamino-4′-N′-methylstilbazolium p-aminobenzenesulfonate, DSAS: Yield 72%; ^{1}H NMR (300 MHz, DMSO-d_6) δ [ppm]: 8.68 (d, 2H, J = 6.9 Hz, C_5H_4N), 8.04 (d, 2H, J = 6.9 Hz, C_5H_4N), 7.92 (d, 1H, J = 16.2 Hz, CH), 7.60 (d, 2H, J = 9.0 Hz, C_6H_4), 7.25 (d, 2H, J = 8.4 Hz, $C_6H_4SO_3^-$), 7.18 (d, 1H, J = 16.2 Hz, CH), 6.79 (d, 2H, J = 9.0 Hz, C_6H_4), 6.44 (d, 2H, J = 8.4 Hz, $C_6H_4SO_3^-$), 5.14 (s, 2H, NH_2), 4.16 (s, 3H, Me), 3.02 (s, 6H, NMe_2). Anal. calcd. for $C_{22}H_{25}N_3O_3S$: C, 64.21; H, 6.12; N, 10.21. Found: C, 63.93; H, 6.27; N, 10.17.

4-N,N-Dimethylamino-4′-N′-methylstilbazolium p-dimethylaminobenzenesulfonate, DSMAS: Yield 63%; ^{1}H NMR (300 MHz, DMSO-d_6) δ [ppm]: 8.68 (d, 2H, J = 6.3 Hz, C_5H_4N), 8.04 (d, 2H, J = 6.0 Hz, C_5H_4N), 7.92 (d, 1H, J = 16.2 Hz, CH), 7.60 (d, 2H, J = 8.4 Hz, C_6H_4), 7.40 (d, 2H, J = 8.4 Hz, $C_6H_4SO_3^-$), 7.18 (d, 1H, J = 16.2 Hz, CH), 6.79 (d, 2H, J = 8.4 Hz, C_6H_4), 6.60 (d, 2H, J = 8.4 Hz, $C_6H_4SO_3^-$), 4.16 (s, 3H, Me), 3.02 (s, 6H, NMe_2), 2.88 (s, 6H, NMe_2). Anal. calcd. for $C_{24}H_{29}N_3O_3S$: C, 65.58; H, 6.65; N, 9.56. Found: C, 65.57; H, 6.77; N, 9.58.

SHG Measurements: The idler wave at a center wavelength of 1907 nm from an optical parametric amplifier (TOPAS, from Light Conversion Ltd.) was pumped by an amplified Ti:sapphire laser (Clark MXR Inc , CPA 2001). Typical pulse energy and pulse duration were 50 μJ and 150 fs (full width at half maximum), respectively. The backscattered light at the second-harmonic wavelength (953.5 nm) was detected with a silicon photodiode, which was not sensitive to the fundamental wavelength. The diode signal was averaged over 100 pulses and integrated with a digital oscilloscope (LeCroy, LC564). Contributions from third-harmonic generation (635.6 nm) were eliminated by appropriate filters.

Crystal Growth: The experiments were performed in a constant temperature bath of controlled stability ±0.01 °C [14]. The solutions were prepared using methanol as the solvent and saturated at 48 °C. After filtering using 0.2 μm porosity Millipore filters, they were preheated to 50 °C for 24 h in sealed crystallizer tubes. This procedure was performed to ensure that all ingredients were dissolved. The programmed cooling rate was 0.3 °C day^{-1}.

X-ray Crystal Structure of DSMOS: Crystal data at 263(2) K for $4(C_{16}N_2H_{19})$ $4(C_7H_7O_4S)$, [M_r = 1706.07] triclinic, space group $P1$, Dc = 1.348 g cm^{-3}, Z = 1, a = 10.6197(5) Å, b = 11.0315(5) Å, c = 18.5956(9) Å, V = 2101.31(17) Å^3. The crystal's dimensions were approximately 0.3 mm × 0.3 mm × 0.3 mm. The necessary data for structural analysis were obtained using a Bruker-Nonius Kappa-CCD (charge-coupled device) diffractometer equipped with a graphite monochromated Mo Kα radiation (λ = 0.7107 Å) at 263 K. The structure was solved by direct methods [15], and refined by full-matrix least-squares analysis including an isotropic extinction correction [16]. All heavy atoms were refined anisotropically (hydrogen atoms isotropic, whereby hydrogen atom positions are based on stereochemical considerations). The final $R(F)$ = 0.0573, $wR(F^2)$ = 0.1464 for 1082 parameters and 8688 reflections with $I > 2\sigma(I)$ and $2.96° < \theta < 26.01°$. CCDC-249496 contains the supplementary crystallographic data for this paper. These data can be obtained free of charge from The Cambridge Crystallographic Data Centre via www.ccdc.cam.ac.uk/data_request/cif.

Received: January 21, 2005

[1] C. Bosshard, K. Sutter, P. Prêtre, J. Hulliger, M. Flörsheimer, P. Kaatz, P. Günter, *Organic Nonlinear Optical Materials, Advances in Nonlinear Optics*, Vol. 1, Gordon and Breach, Amsterdam **1995**.

[2] D. S. Chemla, J. Zyss, *Nonlinear Optical Properties of Organic Molecules and Crystals*, Vols. 1,2, Academic Press, Orlando, FL **1987**.

[3] H. S. Nalwa, S. Miyata, *Nonlinear Optics of Organic Molecules and Polymers*, CRC Press, Boca Raton, FL **1997**.

[4] G. R. Meredith, in *Nonlinear Optical Properties of Organic and Polymeric Materials* (Ed: D. J. Williams), ACS Symposium Series 233, American Chemical Society, Washington, DC **1983**, pp. 27–56.

[5] B. J. Coe, J. A. Harris, A. K. Clays, G. Olbrechts, A. Persoons, J. T. Hupp, R. C. Johnson, S. J. Coles, M. B. Hursthouse, K. Nakatani, *Adv. Funct. Mater.* **2002**, *12*, 110.

[6] S. R. Marder, J. W. Perry, W. P. Schaefer, *Science* **1989**, *245*, 626.

 © 2005 WILEY-VCH Verlag GmbH & Co. KGaA, Weinheim

[7] H. Adachi, Y. Takahashi, J. Yabuzaki, Y. Mori, T. Sasaki, *J. Cryst. Growth* **1999**, *198*, 568.
[8] F. Pan, M. S. Wong, C. Bosshard, P. Günter, *Adv. Mater.* **1996**, *8*, 592.
[9] F. Pan, G. Knopfle, C. Bosshard, S. Follonier, R. Spreiter, M. S. Wong, P. Günter, *Appl. Phys. Lett.* **1996**, *69*, 13.
[10] S. R. Marder, J. W. Perry, W. P. Schaefer, *Chem. Mater.* **1994**, *6*, 1137.
[11] M. H. Carr, H. P. Brown, *J. Am. Chem. Soc.* **1947**, *69*, 1170.
[12] S. K. Kurtz, T. T. Perry, *J. Appl. Phys.* **1968**, *39*, 3798.
[13] M. S. Wong, F. Pan, M. Bosch, R. Spreiter, C. Bosshard, P. Günter, *J. Opt. Soc. Am.* **1998**, *15*, 426.
[14] S. Manette, M. Ehrensperger, C. Bosshard, P. Günter, *C. R. Phys.* **2002**, *3*, 449.
[15] A. Altomare, M. Burla, M. Camalli, G. Cascarano, C. Giacovazzo, A. Guagliardi, A. G. G. Moliterni, G. Polidori, R. Spagna, *J. Appl. Crystallogr.* **1999**, *32*, 115.
[16] G. M. Sheldrick, *SHELXL-97 Program for the Refinement of Crystal Structures*, University of Göttingen, Germany **1997**.

 © 2005 WILEY-VCH Verlag GmbH & Co. KGaA, Weinheim